J. Phys. B: At. Mol. Opt. Phys. **26** (1993) 2795–2810. Printed in the UK

Photoionization of Kr near the 4s threshold: I. Experiment and *LS* coupling theory

H Schmoranzer†, A Ehresmann†, F Vollweiler†, V L Sukhorukov‡, B M Lagutin‡, I D Petrov‡, K H Schartner§ and B Möbus§

† Fachbereich Physik, Universität Kaiserlautern, D-67653 Kaiserlautern, Federal Republic of Germany

‡ Rostov State University, Rostov-on-Don 344017, Russia

§ I Physikalisches Institut, Universität Giessen, D-35392 Giessen, Federal Republic of Germany

Received 21 December 1992, in final form 26 April 1993

Abstract. Absolute cross sections for the transitions of the Kr atom into the $4s^1$ and $4p^4nl$ states of the Kr^+ ion were measured in the 4s-electron threshold region by photon-induced fluorescence spectroscopy (PIFS). The cross sections for the transitions of the Kr atom into the $4s^1$ and $4p^4nl$ states were also calculated, as well as the $4p^4nln'l'$ doubly excited states, in the frame of *LS*-coupling many-body technique. The cross sections of the doubly-excited atomic states were used to illustrate the pronounced contributions of the latter to the photoionization process, evident from the measurements. The comparison of theory and experiment led to conclusions about the origin of the main features observed in the experiment.

1. Introduction

Single-photon excitation of ionic states (satellites), populated when one electron is emitted while another is excited simultaneously, is a manifestation of electron correlations in atoms. Thus the knowledge of cross sections for the population of satellite states may be a key for the understanding of the interactions within a system of many electrons, regarding the interactions between two single electrons as well known (Amusia and Cherepkov 1975, Wijesundera and Kelly 1989, Sukhorukov *et al* 1991).

In view of these fundamental aspects, a lot of experimental investigations were performed recently on Ne (Schartner *et al* 1990, Hall *et al* 1991, Wills *et al* 1990b, Becker *et al* 1986), Ar (Schartner *et al* 1988, Hall *et al* 1989, Wills *et al* 1989, Becker *et al* 1986), Kr (Wills *et al* 1990a, Schmoranzer *et al* 1990, Hall *et al* 1990) and Xe (Hall *et al* 1990, Wills *et al* 1990a, Schartner *et al* 1989) using photoelectron spectroscopy (PES) and photo-induced fluorescence spectroscopy (PIFS). However, mostly relative cross sections were measured and absolute values were determined in a few cases only. In krypton, for example, the absolute 4s-electron ionization cross section was measured experimentally to our knowledge only by Samson and Gardner (1974) and by Aksela *et al* (1987) and no data are available for absolute satellite-state excitation cross sections.

On the theoretical side, only a few absolute Kr 4s-electron ionization cross section calculations were performed (Kennedy and Manson 1972, Amusia and Cherepkov 1975, Sukhorukov *et al* 1991, Petrov and Sukhorukov 1991, Huang *et al* 1981). Up to now,

0953-4075/93/172795+16$07.50

no attempt has been made to calculate cross sections for the population of Kr II satellite states as well as for the population of doubly excited states in Kr I.

In the present paper, the many-body theory was used to calculate absolute cross sections of the Kr 4s-electron photoionization and the excitation of satellite states near the Kr 4s ionization threshold. The influence of the autoionization of doubly-excited atomic states on these cross sections was not yet included, but as a first step, cross sections for the excitation of these doubly-excited states were calculated. Some principles of the method will be demonstrated by calculating different ionization potentials which were used for the calculations of the cross section.

The PIFS was used in the present work for the observation of new satellite excitation cross sections. Furthermore absolute values for the Kr 4s ionization cross section and—for the first time—for satellite state excitation cross sections were estimated in an energy region from the respective thresholds to approximately 3 eV above threshold.

2. Experimental

2.1. Determination of absolute cross sections by means of PIFS

2.1.1. General method. PIFS and its applications to the determination of relative and absolute cross sections have been extensively described previously (Shartner *et al* 1988, 1989, 1990, Schmoranzer *et al* 1990). Thus we mention only the most important experimental parameters of our present investigation and, in particular, the method of determining absolute cross sections of the Kr 4s ionization and the corresponding satellite level excitation.

Monochromatized synchrotron radiation from the storage ring BESSY, Berlin, with a typical bandwidth of 150 meV was focused into a differentially pumped target cell. The Kr gas pressure in the target cell was held at a constant value of 13×10^{-2} mbar. The flux of the exciting radiation was determined using the time integrated secondary-electron current emitted from the Al cathode of a Faraday cup. The quantum efficiency of this device was obtained by comparison with a Faraday cup calibrated by the NIST (Möbus 1988). The fluorescence radiation emitted in a direction perpendicular to the photon beam of the exciting radiation was dispersed by a 1 m McPherson monochromator and recorded by a position-sensitive detector which was mounted in the focal plane of the monochromator. An entrance slit width of 100 μm resulted in a resolution of less than 2 Å. A typical spectrum of Kr in the fluorescence range between 75 nm and 95 nm is shown in figure 1. The relative quantum efficiency of the monochromator–detector system was determined using cross sections for electron-impact induced line radiation and branching ratios within multiplets (Schartner *et al* 1988, 1991). Absolute cross sections were obtained from a comparison of the fluorescence intensities of the Kr II $4s^14p^6\ ^2S_{1/2} \rightarrow 4s^24p^5\ ^2P_{1/2,3/2}$ transitions with the fluorescence intensities of the Ar II $3s^13p^6\ ^2S_{1/2} \rightarrow 3s^23p^5\ ^2P_{1/2,3/2}$ transitions where absolute cross sections are known.

The spectra for the comparison of Ar and Kr were recorded during one and the same filling of the electron storage ring in order to minimize fluorescence intensity variations caused by changing positions of the exciting photon beam.

2.1.2. Choice of states for absolute cross section determinations. To obtain absolute cross sections by means of PIFS, we have to consider those states which decay exclusively by fluorescent channels. Obviously, all of these channels have to be observed. Due to the

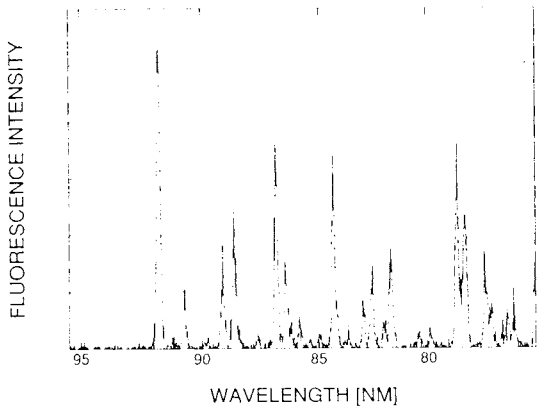

Figure 1. Kr fluorescence spectrum between 75 nm and 95 nm at an exciting photon energy of 33 eV.

characteristics of our present monochromator–detector combination such states have to be chosen which emit fluorescence radiation in the wavelength region between approximately 500 Å and 1000 Å. In the case of Kr, these are the Kr II $4s^1 4p^6\ ^2S_{1/2}$ state and the Kr II satellite states of the $4s^2 4p^4$ 4d or $4s^2 4p^4$ 5s configurations.

2.1.3. Cascade effects. As a disadvantage of the employed method, the possible occurence of cascade effects has to be considered. To examine cascade effects within the first 3 eV of the cross sections from the corresponding threshold on, some of our measurements were compared with published cascade-free PES results (Hall *et al* 1990): figure 2 shows absolute cross sections of the Kr II states $(^3P)5s\ ^4P_{5/2}$, $(^3P)5s\ ^4P_{1/2}$ and $(^3P)4d\ ^4D_{3/2}$ determined by PIFS. The same cross sections have been measured on a relative scale using PES by Hall *et al* (1990). In spite of our larger bandwidth of approximately 150 meV (Hall *et al* (1990): 100 meV) qualitatively the same features were observed in the first 2eV above threshold by PIFS as by PES.

However, cascade effects were observed at higher energies. For the $(^3P)5s\ ^4P_{5/2}$ satellite state, e.g., there is a sudden increase in the cross section at approximately 30.6 eV. This increase is due to the opening of a couple of strong cascade channels. The strongest of these cascade channels for the $(^3P)5s\ ^4P_{5/2}$ satellite state are (Striganov and

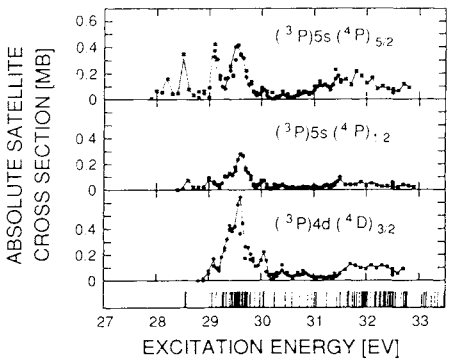

Figure 2. Absolute cross sections for excitation of Kr II satellite states measured by PIFS.

Table 1. Proposed assignments for the fluorescent transitions at 864.812 Å and 826.432 Å according to Striganov and Sventitskij (1968) and Kelly (1987).

Fluorescence line (Å)	Transitions: Striganov and Sventitskij (1968)	Transitions: Kelly (1987)	Threshold energy (eV)
864.812	$(^3P)4d\ ^4D_{3/2} \rightarrow 4p^5\ ^2P^o_{1/2}$	$(^3P)4d\ ^4D_{3/2} \rightarrow 4p^5\ ^2P^o_{1/2}$	28.99
	$(^3P)5s\ ^2P_{1/2} \rightarrow 4p^5\ ^2P^o_{1/2}$		28.99
826.432	$(^3P)5s\ ^2P_{1/2} \rightarrow 4P^5\ ^2P^o_{3/2}$	$(^3P)5s\ ^2P_{1/2} \rightarrow 4p^5\ ^2P^o_{3/2}$	28.99
	$(^3P)4d\ ^4D_{3/2} \rightarrow 4p^5\ ^2P^o_{3/2}$		28.99

Sventitskij 1968):

$$(^3P)5p\ ^4D_{5/2} \rightarrow (^3P)5s\ ^4P_{5/2} + 4739\ \text{Å}\ (E_{th}((^3P)5p\ ^4D_{5/2}) = 30.60\ \text{eV})$$

$$(^3P)5p\ ^4P_{3/2} \rightarrow (^3P)5s\ ^4P_{5/2} + 4658\ \text{Å}\ (E_{th}((^3P)5p\ ^4P_{3/2}) = 30.65\ \text{eV})$$

$$(^3P)5p\ ^4D_{7/2} \rightarrow (^3P)5s\ ^4P_{5/2} + 4355\ \text{Å}\ (E_{th}((^3P)5p\ ^4D_{7/2}) = 30.83\ \text{eV})$$

where E_{th} is the threshold energy of the corresponding ionic state.

The same analysis can be made for all other satellite states which have been observable in the present experiment. It should be emphasized, however, that cascades are not observable within the first 2 eV of the determined satellite cross sections. For the 4s ionization cross sections, the situation is better because the states of the configuration $4s^14p^5\ ns/nd$ which could give rise to cascade transitions have even higher threshold energies.

2.2. Experimental results and discussion

2.2.1. State assignments. The assignments of initial and final states of certain transitions are sometimes ambiguous when comparing different tables (Striganov and Sventitskij 1968, Kelly 1987). Thus the consistency of the literature data has to be checked carefully.

A first case of ambiguous state assignment is connected with lines at 864.812 Å and 826.432 Å. Table 1 shows the different assignments of the initial states according to Striganov and Sventitskij (1968) and Kelly (1987). Kelly gives two different initial states for the two fluorescence lines while the threshold energies are the same for both proposed initial states, offering no criterion for an experimental decision. However, the observed intensity ratio of the two lines as a function of photon energy is constant, suggesting that the emission stems from one single initial state. According to Striganov and Sventitskij (1968) two possible assignments are listed for this state. A comparison of its presented excitation cross section with a PES-measured cross section of a state assigned $(^3P)4d\ ^4D_{3/2}$ in the work of Hall *et al* (1990) having the same threshold reveals similar features (see figure 2). Thus, for reasons of consistency with existing literature data, this state will be referred to as $(^3P)4d\ ^4D_{3/2}$†.

† However, in the work of Hall *et al* (1990) there is also an ambiguity in assigning this state because the state c of figure 3, in Hall *et al* (1990), is assigned $(^3P)4d\ ^4D_{3/2}$ whereas the same state c in table 1, in the same paper, is assigned $(^3P)4d\ ^4D_{7/2,5/2}$.

Table 2. Proposed assignments for the fluorescent transitions at 818.149 Å and 783.724 Å according to Striganov and Sventitskij (1968) and Kelly (1987). The erroneous assignment $(^1D)5s\ ^2S_{3/2}$ in Striganov and Sventitskij (1968) has been replaced by $(^1D)5s\ ^2D_{3/2}$ for the transition at 818.149 Å (see text).

Fluorescence wavelength (Å)	Transitions		Threshold energy (eV)
	Striganov and Sventitskij (1968)	Kelly (1987)	
818.149	$(^1D)5s\ ^2D_{3/2}\rightarrow 4p^5\ ^2P^o_{1/2}$	$(^1D)5s\ ^2D_{3/2}\rightarrow 4p^5\ ^2P^o_{1/2}$	29.81
783.724	$(^1D)5s\ ^2D_{3/2}\rightarrow 4p^5\ ^2P^o_{3/2}$		29.81
	$(^3P)4d\ ^2D_{3/2}\rightarrow 4p^5\ ^2P^o_{1/2}$	$(^3P)4d\ ^4P_{3/2}\rightarrow 4p^5\ ^2P^o_{1/2}$	30.47

A second case of assignment ambiguity concerns fluorescence lines at 818.149 Å and 783.724 Å. Table 2 shows the assignments from the two data sources. Obviously there is a misprint in the assignment of the initial state of the 818.149 Å line in Striganov and Sventitskij (1968). The $^2S_{3/2}$ term symbol has to be replaced by $^2D_{3/2}$. Thus according to Striganov and Sventitskij (1968) the initial state $(^1D)5s\ ^2D_{3/2}$ has fluorescent transitions at 818.149 Å and 783.724 Å. However, the line at 783.724 Å is blended by another transition which has a threshold at 30.47 eV. The intensity of the 783.724 Å line as a function of incident photon energy was found to increase slightly at approximately 29.8 eV (which is the threshold energy of the $(^1D)5s\ ^2D_{3/2}$ state). A 3.5 times stronger increase in intensity was observed at approximately 30.5 eV which corresponds to the decay of the state with a threshold energy of 30.47 eV. Thus at energies higher than 30.47 eV, the contribution of the decay of the state $(^1D)5s\ ^2D_{3/2}$ to the intensity of the line at 783.724 Å was assumed to be negligible.

2.2.2. Branching ratios. The branching of the decay of various Kr II satellite states to the $4p^5\ ^3P^o_{3/2}$ and to the $4p^5\ ^3P^o_{1/2}$ state was also investigated. This branching ratio $R(i)$ of the initial state i was obtained according to

$$R(i)=\frac{I_{obs}(i\rightarrow {}^2P^o_{3/2})/\eta(i\rightarrow {}^2P^o_{3/2})}{I_{obs}(i\rightarrow {}^2P^o_{1/2})/\eta(i\rightarrow {}^2P^o_{1/2})} \tag{1}$$

where $I_{obs}(i\rightarrow {}^2P^o_{3/2})$ and $I_{obs}(i\rightarrow {}^2P^o_{1/2})$ are the observed fluorescence intensities of the transitions to the $^2P^o_{3/2}$ and $^2P^o_{1/2}$ states, respectively, and $\eta(i\rightarrow {}^2P^o_J)$ are the relative quantum efficiencies of our monochromator–detector combination (Schartner *et al* 1988, 1991) for the corresponding transition wavelengths. The results are shown in table 3.

Table 3. Branching ratios for the decay of some satellite states in the two possible fluorescent channels.

Initial state assignment	Transition wavelength (Å)		Branching ratio $^2P_{3/2}:{}^2P_{1/2}$
	to $^2P_{3/2}$	to $^2P_{1/2}$	
$(^3P)5s\ ^4P_{1/2}$	850.319	891.004	0.06
$(^3P)5s\ ^4P_{3/2}$	868.871	911.394	18.2
$(^3P)5s\ ^2P_{3/2}$	844.058	884.144	5.6
$(^3P)4d\ ^4D_{3/2}$	826.432	864.812	1.9
$(^3P)4d\ ^4D_{1/2}$	821.154	859.037	0.9

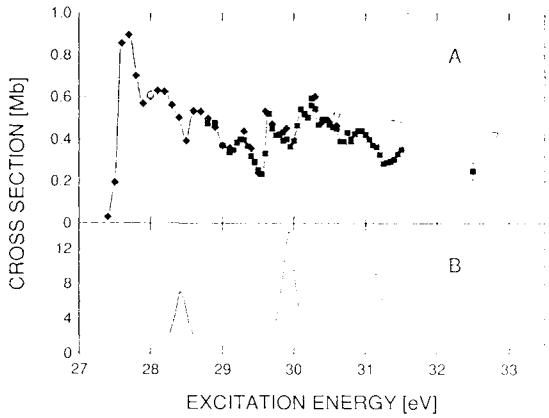

Figure 3. (a) 4s-electron ionization cross section as a function of exciting photon energy near threshold. Experiment: ◆, ■, present data, different runs (points are connected by a full curve, where necessary, to guide the eyes); theory: ○, Samson and Gardner (1974); - - - -, Amusia and Cherepkov (1975); ——, present calculations. (b) Calculated excitation cross sections for doubly excited Kr I states represented as the sum of the cross sections of table 7 convoluted by Lorentzians of 0.2 eV width (FWHM).

The uncertainty is about 40% which results mainly from the uncertainty of the relative quantum efficiency. Both the unsystematical behaviour of the branching ratios and the intercombination transitions between quartet and doublet states demonstrate the breakdown of the *LS*-coupling scheme.

2.2.3. 4s-electron ionization cross section. Figure 3(a) shows the PIFS-determined absolute 4s ionization cross section for krypton in an energy range from threshold up to 31.5 eV in comparison with other experimental (Samson and Gardner 1974) and theoretical (Amusia and Cherepkov 1975) results and with our calculations. Figure 3(b) displays the sum of calculated excitation cross sections of doubly excited Kr I states. The calculations will be described below. Our experimental cross section is in excellent agreement with the cross section determined by Samson and Gardner (1974). A detailed discussion of the different curves in figure 3 will be given in section 4.3.

2.2.4. Excitation cross sections of satellite states. In figures 2, 4 and 5, PIFS-measured excitation cross sections for Kr II satellite states are presented for an excitation energy interval of about 3 eV starting from the corresponding threshold. Note that all of these cross sections have been recorded perpendicularly to the incident photon beam. Since there are no experimental data for the possible alignment of the satellite states for $J > \frac{1}{2}$, the corresponding cross sections have not been corrected for this effect. Neglecting alignment effects, our results have an error of about 40% on the absolute scale and about 20% on the relative scale. A typical error bar is drawn for each cross section of figures 3, 4 and 5. At the bottom of figures 2, 4 and 5 experimental positions of resonances in the absorption spectrum of Kr I have been indicated by bars (Codling and Madden 1972). The resonances were not assigned so far, but in analogy to the corresponding cases in Ne and Ar most of them have to belong to doubly excited states. Obviously, the satellite-state cross sections are only influenced by the autoionization of the doubly excited Kr I states within approximately the first two eV starting at threshold. The absolute cross sections are all of the same order of magnitude (approximately 0.2-0.6 Mb when influenced by the doubly-excited Kr I states).

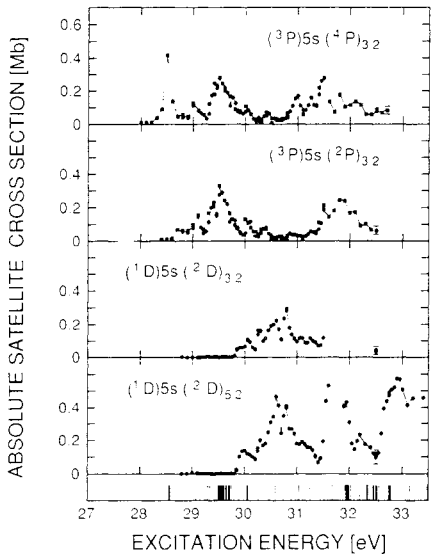

Figure 4. Measured absolute cross section for population of satellite states with an outer 5s electron.

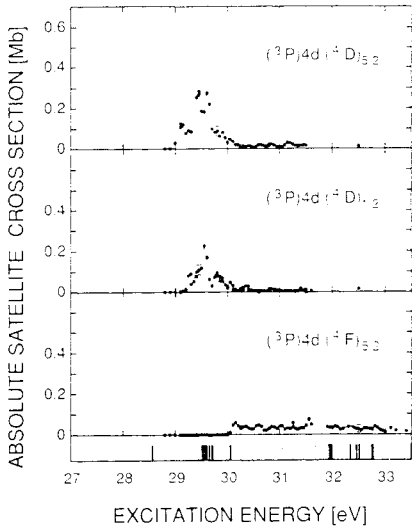

Figure 5. Measured absolute cross section for population of satellite states with an outer 4d electron.

3. Theory

3.1. Technique of calculations

3.1.1. General method. To calculate the Kr 4s ionization cross section and Kr II satellite cross sections a combination of the configuration interaction technique and many-body perturbation theory was used. For the calculation of energies and total wavefunctions in Kr the configuration interaction technique was used with $4s^{-1}(^2S)$ and $4p^{-2}\,nl\,(LS)$

basis states. It was shown by Sukhorukov *et al* (1992) for the case of Ar that the construction of secular matrices on these states requires some semiempirical changes of both diagonal and non-diagonal matrix elements to describe experimental energies and cross sections accurately. However, in many cases the inclusion of interactions with highly excited configurations leads to an improvement of the theoretical results without semiempirical parameters (Rajnak and Wybourne 1963, Demekhin *et al* 1979). Therefore we shall calculate energy levels and cross sections including such highly excited configurations.

In the following sections we shall first demonstrate our technique by calculating the 2p, 3s, 3p, 3d, 4s and 4p ionization potentials (IP) of Kr showing, where possible, the consecutive steps of improvement or the possible ways of proceeding further.

3.2.1. Average configuration energies. To calculate the IPs, the total energies of the ground state and singly ionized states of Kr were evaluated in the self-consistent non-relativistic (superscript 'nr') Hartree–Fock (HF) approximation. The accuracy of the calculations was checked by evaluating the ratio of potential to kinetic energy (virial theorem parameter). Energies were accurate in this sense within 0.01 eV. The calculated total energies $E^{\mathrm{nr}}_{\mathrm{HF}}(i)$ were used to determine the IP by

$$IP^{\mathrm{nr}}_{\mathrm{HF}}(i) = E^{\mathrm{nr}}_{\mathrm{HF}} - E^{\mathrm{nr}}_{\mathrm{HF}}(0) \tag{2}$$

where '0' denotes the Kr I ground state and 'i' the configuration with an i-shell vacancy. A total energy of $E^{\mathrm{nr}}_{\mathrm{HF}}(0) = -5504.110$ Ryd was calculated and the conversion factor of 1 Ryd = 13.6058 eV was used. Table 4 shows the results together with experimental IPs ($\mathrm{IP_{EXP}}$). $\mathrm{IP_{EXP}}$ is a mean value derived from the data of Sevier (1979) by considering the statistical weights of the individual multiplet components. In the same table relativistic ionization potentials $\mathrm{IP_{HF}}$ are presented which were calculated using non-relativistic atomic orbitals and a relativistic Hamiltonian in Breit form (Bethe and Salpeter 1957).

In this approximation the ground state energy is $E^{\mathrm{r}}_{\mathrm{HF}}(0) = -5573.218$ Ryd. The agreement between experiment and theory is satisfactory both for inner shells and valence shells. Therefore all further calculations were performed in this relativistic approximation and we will omit the superscript 'r' in the following formulae. The differences between $\mathrm{IP_{EXP}}$ and $\mathrm{IP_{HF}}$ are of the order of a few eV and have no systematic trend. To reduce them we consider the influence of highly excited configurations by the second-order perturbation theory (PT). Therefore the correction of the energies is

Table 4. Ionization potentials (in eV) of some Kr core shells.

nl	$\mathrm{IP_{EXP}}$	IP^{nr}_{HF}	$\mathrm{IP_{HF}}$	$\mathrm{IP_{HF}} - \mathrm{IP_{EXP}}$	$C(nl) - C(0)$	$\mathrm{IP_2} - \mathrm{IP_{EXP}}$	$\mathrm{IP_{theor}}$
2p	1696	1684.87	1697.30	1.30	0.11	1.41	1696.02
3s	292.8	286.24	295.57	2.77	−1.84	0.93	292.34
3p	216.7	217.72	219.71	3.01	−1.24	1.77	217.08
3d	94.3	94.78	92.68	−1.62	3.15	1.53	94.44
4s	27.51	30.11	30.91	3.46	1.28[a]	4.74[a]	27.56[b]
4p	14.21	13.27	13.24	−0.97	2.29	1.32	14.14

[a] $4p^4\{d\}$ and $4p^4\{s\}$ channels are excluded.
[b] $4p^4\{d\}$ and $4p^4\{s\}$ channels are included by diagonalization technique.

described by

$$C(i)=\frac{1}{g(i)}\sum_{x m_x m_i}\frac{\langle m_i i \mid H-E \mid m_x x\rangle\langle m_x x \mid H-E \mid m_i i\rangle}{E(m_i i)-E(m_x x)} \tag{3}$$

where Σ_x denotes the summation over discrete-state configurations and integration over continuum ones, m_i and m_x are the sets of quantum numbers of the given (i) and the excited (x) configurations; $g(i)$ is the statistical weight of configuration 'i'. H is the total Hamiltonian of the atom.

The summation in equation (3) may be simplified considerably by neglecting the multiplet splitting of the i and x configurations in the denominator (i.e. we assume that $E(m_i i)-E(m_x x)=E(i)-E(x)$, where $E(i)$ and $E(x)$ are the average configuration energies). In this case the denominator can be taken out of the sum and the summation can be carried out analytically (Bauche *et al* 1988, Karazija 1991).

Numerical calculations of $C(0)$ and $C(i)$ were performed including {s}, {p}, {d}, {f}, {g} and {h} virtual channels where in each channel $\{l\}$ both two discrete states and continuum states in the range between 0 and 400 Ryd were contained. The second-order PT (subscript '2') corrected IPS are then given by

$$\mathrm{IP}_2(i)=\mathrm{IP}_{\mathrm{HF}}(i)+C(i)-C(0) \tag{4}$$

with a many-body correction to the ground state of $C(0)=-48.28$ eV. $C(i)-C(0)$ and the differences between experiemental ($\mathrm{IP}_{\mathrm{EXP}}$) and corrected ionization potentials ($\mathrm{IP}_2(i)$) are shown in table 4, too. Except for the 4s case, the differences $\mathrm{IP}_2(i)-\mathrm{IP}_{\mathrm{EXP}}(i)$ have similar values for all shells. The 4s case will be discussed in detail below. This difference arises possibly from the neglection of higher orders of PT which usually decrease the results of correlation energy calculations in lower orders of PT (Rajnak and Wybourne 1963).

With a mean value of 1.39 ± 0.27 eV for $\mathrm{IP}_2(i)-\mathrm{IP}_{\mathrm{EXP}}(i)$ we may now estimate a mean value $\bar{\Delta}$ of higher-order PT corrections for a single electron pair by considering, for Kr, only the 32 electrons $2p^6 3s^2 3p^6 3d^{10} 4s^2 4p^6$ which were found to yield the main contributions to $C(i)$

$$\bar{\Delta}=\frac{1.39}{\binom{32}{2}-\binom{31}{2}}. \tag{5}$$

$\binom{32}{2}-\binom{31}{2}$ is the difference in the number of electron pairs in systems with 32 and 31 electrons. Table 4 shows the theoretical IPS ($\mathrm{IP}_{\mathrm{theor}}$) corrected by $\bar{\Delta}\cdot[\binom{32}{2}-\binom{31}{2}]$. Theory and experiment agree within 0.3 eV or less.

Using the described procedure the IPS of $4p^4 nl$ and $4p^4$ configurations were calculated (see table 5). The correction due to higher orders of PT was

$$\Delta\mathrm{IP}^N_{\mathrm{HPT}}=\bar{\Delta}\cdot[\binom{32}{2}-\binom{32-N}{2}] \tag{6}$$

Table 5. Ionization potentials (in eV) of Kr levels which strongly interact with the $4s^{-1}$ level. The interactions between the states listed in the table are excluded.

Configuration	$\mathrm{IP}_{\mathrm{HF}}$	$C(i)-C(0)$	$\mathrm{IP}_{\mathrm{theor}}$
$4p^{-2}4d$	29.69	4.11	31.08
5d	33.42	4.58	35.28
5s	27.73	4.15	29.16
5p	30.22	4.34	31.84
$4p^{-2}$	37.39	4.64	39.31

where N is the number of core vacancies. $4p^4nl$ configurations were treated with $N=2$ because the interactions of the outer nl electron with the core are much less than the interactions of the core electrons with each other. The comparison between the centre-of-gravity energy from the tables of Moore (1971) for the $4p^4$ configuration ($IP_{EXP}(4p^4) = 39.61$ eV) and the calculated energy ($IP_{theor}(4p^4) = 39.31$ eV) reveals a difference of 0.3 eV, showing the accuracy of the technique employed.

We now return to the special case of the 4s-electron ionization. The significantly larger difference $IP_2(4s) - IP_{EXP}(4s)$ is caused by neglecting the 4p4p–4s$\{l\}$ interactions. As these interactions are known to be large, they were taken into account by diagonalizing the corresponding secular matrix. The results for the 4s IP without and with inclusion of 4p4p–4s$\{l\}$ interactions are also shown in table 4.

3.3. The strength of the Coulomb interaction

As mentioned above, many-electron correlations decrease the strength of the Coulomb interaction calculated in the HF approximation. We calculated this decrease with the use of the non-diagonal terms of equation (3) (i.e. the non-diagonal terms of second-order PT) with HF wavefunctions for the special case of 4p4p − 4s4d interaction. The corrections to the matrix element $\langle 4s^1 4p^6\ ^2S \mid H^{ee} \mid 4s^2 4p^4(^1D)4d\ ^2S\rangle$, which is equal to −4.68 eV in HF approximation, are listed in table 6. The most significant corrections are due to excitations to states with the same principal quantum number. For this reason, higher-order PT corrections (which represent the effect of perturbed perturbing states on the interaction) can be included by iteration. For the 4p4p–4s4d interaction, the decrease factor was 1.54 and 1.38 before and after the iteration procedure, respectively. For the 4p4p–4s5d interaction, the iteration yielded a factor of 1.40. Therefore we took a factor of 1.38 for decreasing the 4p4p–4s$\{l\}$ Coulomb interaction.

The Coulomb interaction was to be decreased not only between configurations but also within a configuration (Rajnak and Wybourne 1963, Demekhin *et al* 1979). The technique described above is capable of calculating these corrections but this would be rather time-consuming. However, this value can be easily extracted from a comparison between calculated and measured (Moore 1971) energies of the $4p^4$ multiplet. After decreasing the 4p–4p Coulomb interaction by a factor of 1.20 we obtained good agreement between experiment and theory. Therefore Coulomb interactions within each configuration were decreased by a factor of 1.20 which is, besides $\bar{\Delta}$, the only empirical factor of our calculations.

Table 6. Correlation corrections in eV to the $\langle 4s^1 4p^6\ ^2S \mid H^{ee} \mid 4s^2 4p^4(^1D)4d\ ^2S\rangle$ matrix element (see text).

Configuration	Correction	Configuration	Correction
$4s^{-1}4p^{-2}4d^2$	0.46	$3d^{-1}4s^{-1}4p^{-1}4d\{f\}$	0.24
$4s^{-1}4p^{-2}\{d\}\{d\}$[a]	0.54	$\{p\}$	0.02
$\{f\}\{f\}$	0.05	$3d^{-1}4p^{-1}\{f\}$	0.07
$\{d\}\{g\}$	0.05	other configurations	0.19
$\{f\}\{h\}$	0.02	total correction	1.64

[a] Without $4s^{-1}4p^{-2}4d^2$.

3.4. The multiplet structure of excited atomic states

The calculated average-configuration energies and Coulomb-interaction decrease factors were then used to construct the secular matrices for ^{2}S, ^{2}P and ^{2}D Kr ionic terms. In these matrices the basis states $4s^{-1}$, $4p^{-2}\{d\}$ and $4p^{-2}\{s\}$ were included. After the diagonalization of these matrices, the eigenenergies and eigenvectors were obtained. These values were used in the calculations of photoionization cross sections described below.

To calculate the energies of the doubly-excited $4p^4n(s/d)n'p$ ^{1}P states, the IPS of n'p electrons were subtracted from the eigenenergies which were calculated by diagonalizing the secular matrices for ^{2}S, ^{2}P and ^{2}D terms of the Kr ion. The IP(n'p) values were calculated by the same procedure as the IPS of core electrons. For 5p electrons they are equal to 2.58 eV, 2.83 eV and 3.34 eV in $4s^15p$, $4d^44d5p$ and $4p^45s5p$ configurations, respectively. For 6p and 7p electrons, they are 1.28 eV and 0.73 eV in all cases.

3.5. Transition amplitudes

For the calculation of the transition amplitudes we used the electric dipole approximation and the second-order many-body PT. The main difference between the Ar calculations of Sukhorukov *et al* (1992) and the present Kr calculations is the additional consideration of the $\langle 3d \mid r \mid \varepsilon l\rangle$ amplitudes for the evaluation of the $\langle 4s \mid r \mid \varepsilon p\rangle$ amplitudes. Thus the $\langle 4s \mid r \mid \varepsilon p\rangle$ amplitude was calculated according to the scheme:

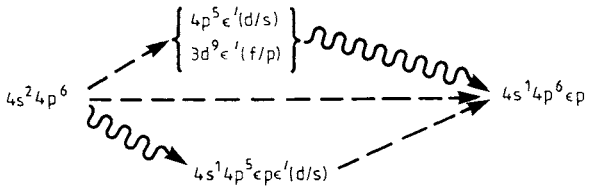

(7)

where dashed lines denote the electric dipole interaction and wavy lines the Coulomb interaction.

The transition amplitudes for the simultaneous ionization and excitation as well as the amplitudes for double excitation were calculated according to

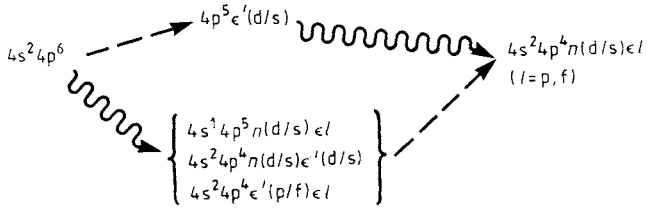

(8)

In the case of double excitation the εl function in (8) has to be replaced by 5p, 6p and 7p orbitals.

The $\langle 4p \mid r \mid \varepsilon'(d/s)\rangle$ amplitudes were calculated by taking into account inner-shell correlations (Amusia and Cherepkov 1975, Sukhorukov *et al* 1992). The $\varepsilon'(d/s)$ and εp orbitals used in the $\langle 4p \mid r \mid \varepsilon'(d/s)\rangle$ and $\langle 4s \mid r \mid \varepsilon p\rangle$ amplitudes, respectively, were obtained by solving the HF equation with frozen-core orbitals (denoted by the subscript '0') of the Kr ground state. The core configurations $4s_0^14p_0^6$ for εp and $4s_0^24p_0^5$ for $\varepsilon'(d/s)$ orbitals were used.

To calculate, for example, the transition amplitude $4s^24p^6 \rightsquigarrow 4s^24p^44d\varepsilon'd \dashrightarrow 4s^24p^44d\varepsilon p$ the divergent matrix element $\langle \varepsilon'd \mid r \mid \varepsilon p\rangle$ was calculated using the same

technique as described, e.g., by Carter and Kelly (1977). According to this technique, the solution of a special kind of inhomogeneous differential equation leads to so-called correlation functions. These functions avoid all divergence problems because of their asymptotic behaviour like $e^{-\alpha r}$.

Since the length and velocity HF cross sections were expected to be different, the velocity form was calculated, too. Very good agreement, i.e. within a few per cent, was found for the majority of transitions considered. In two cases only the discrepancy was larger, for example, about 10%.

4. Theoretical results and final discussion

4.1. 4s-electron ionization cross section

The calculated 4s-electron ionization cross section is presented in figure 6 together with theoretical (Amusia and Cherepkov 1975, Huang *et al* 1981) and experimental results (Samson and Gardner 1974, Aksela *et al* 1987, Lindle *et al* 1987). In the excitation energy region around the cross section minimum all theoretical results show remarkable agreement in the gross features, among themselves as well as with the measurements, considering the fact that Hartree–Fock cross sections (Kennedy and Manson 1972) do not even show a minimum above the 4s threshold. In the near-threshold region (see figure 3), however, our calculated cross section is larger than that of Amusia and Cherepkov (1975) and experimental data (Samson and Gardner 1974 and present data). The probable reason for this discrepancy is the correlational decrease of the $4s^1\{p\}$–$4p^5\{d\}$ Coulomb interaction which was not considered in the present calculation.

In the high-energy region our calculated cross section is smaller than the measurements of Aksela *et al* (1987). The reason for this discrepancy remains unclear. The measurement of Lindle *et al* (1987) at 91.2 eV agrees well with our calculations. The discrepancy between our cross sections and those of Huang *et al* (1981) may be of systematical nature if the interactions between the $4s^{-1}$ and the $4p^{-2}\{s/d\}$ channels

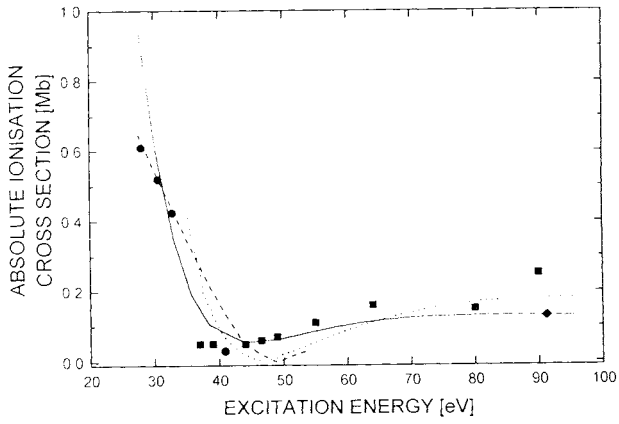

Figure 6. 4s-electron ionization cross section as a function of exciting photon energy. Experiment: ●, Samson and Gardner (1974); ■, Aksela *et al* (1987); ◆, Lindle *et al* (1987). Theory: ---, Amusia and Cherepkov (1975); · · ·, Huang *et al* (1981); ——, present calculations.

were not taken into account by these authors. These interactions lead to a decrease of the cross section by the spectroscopic factors in the high energy region but not near threshold (Sukhorukov *et al* 1985, 1991). In our calculations this decrease factor turned out to be 0.643.

4.2. Satellite lines

The photoionization cross sections of the most strongly populated satellite levels $4p^4(L_0S_0)nl\,(LS)$ are presented in figure 7. The threshold values are larger by a factor

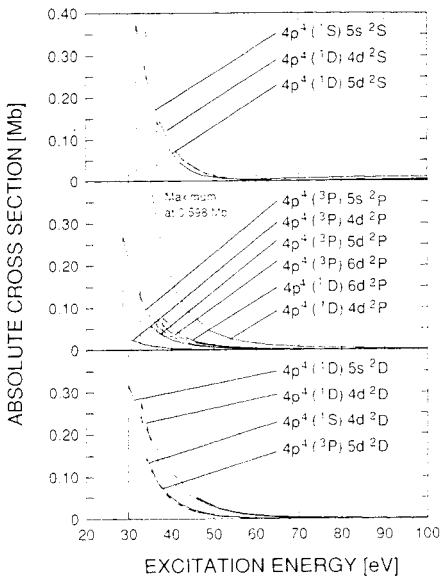

Figure 7. Calculated photoionization cross sections of ^{2}S, ^{2}P and ^{2}D satellite states.

of ~2 than in the corresponding Ar cases (Sukhorukov *et al* 1992). This will be due to the fact that the main contribution of the transition amplitudes is connected with the polarization of the 4p shell. Since the differences between the $4p^4(L_0S_0)nl\,(LS)$ threshold energies and the 4p ionization threshold are approximately by 4 eV smaller than in the corresponding Ar cases the influence of the 4p-shell polarization is much stronger in Kr, resulting in an increase of the satellite cross sections.

A direct comparison of the experimental and theoretical data is difficult because we neglected in the present calculations the autoionization of doubly excited states and the 4p-spin-orbital interaction. Both reasons may lead to significant changes in the results and will be subjected to further theoretical investigations.

4.3. Doubly excited states

In table 7 the calculated oscillator strengths of the strongest transitions into the Kr I $4p^4(L_0S_0)nl\,(LS)np\ ^1$P doubly excited states are presented for Kr II ^{2}S, ^{2}P and ^{2}D parent terms. For each core state, the percentage of the pure basis state for the total eigenvector is given in the row below the basis state. For these states, the calculated energies are shown, too. The sum of all oscillator strengths of table 7 is shown in figure 3(b)

Table 7. Calculated energies, genealogy and oscillator strengths of transitions into doubly excited states of Kr.

Core term ^2S			Core term ^2P			Core term ^2D		
Configuration	Photon energy (eV)	$f(\times 10^{-3})$	Configuration	Photon energy (eV)	$f(\times 10^{-3})$	Configuration	Photon energy (eV)	$f(\times 10^{-3})$
$4s^{-1}$ 5p	24.95	35.69	$4p^4(^3P)5s$ 5p	25.24	13.57	$4p^4(^1D)5s$ 5p	26.42	14.66
64%[a] 6p	26.34	8.28	97% 6p	27.29	2.48	94% 6p	28.47	2.80
7p	26.80	3.37	7p	27.84	0.98	7p	29.02	1.12
$4p^4(^1S)5s$ 5p	28.42	17.76	$4p^4(^3P)4d$ 5p	27.59	1.09	$4p^4(^3P)4d$ 5p	27.92	0.94
89% 6p	30.47	3.40	55% 6p	29.14	0.22	56% 6p	29.50	0.15
7p	31.03	1.34	7p	29.69	0.10	7p	30.05	0.05
$4p^4(^1D)4d$ 5p	31.15	16.84	$4p^4(^1D)4d$ 5p	29.94	26.19	$4p^4(^1D)4d$ 5p	29.91	14.41
54% 6p	32.70	3.45	47% 6p	31.49	5.53	51% 6p	31.46	2.78
7p	33.25	1.34	7p	32.04	2.18	7p	32.01	1.07
$4p^4(^1D)5d$ 5p	33.64	6.89	$4p^4(^3P)6s$ 5p	31.13	0.45	$4p^4(^1S)4d$ 5p	31.14	7.19
75% 6p	35.19	1.41	95% 6p	32.68	0.10	85% 6p	32.69	1.44
7p	35.74	0.55	7p	33.24	0.03	7p	33.24	0.54
$4p^4(^1S)6s$ 5p	34.68	0.52	$4p^4(^3P)5d$ 5p	32.08	2.58	$4p^4(^3P)5d$ 5p	32.25	6.35
79% 6p	36.23	0.10	75% 6p	33.64	0.55	66% 6p	33.80	1.19
7p	36.78	0.05	7p	34.19	0.22	7p	34.35	0.45
			$4p^4(^1D)5d$ 5p	33.12	0.98	$4p^4(^1D)6s$ 5p	32.55	0.10
			56% 6p	34.67	0.20	89% 6p	34.10	0.03
			7p	35.23	0.07	7p	34.66	0.00
						$4p^4(^1D)5d$ 5p	33.19	0.08
						67% 6p	34.74	0.00
						7p	35.29	0.00

[a] Percentage of the basis state in the total eigenvector.

represented as a sum of Lorentzians of 0.2 eV width (FWHM) and a maximum of each amplitude $\sigma_0[\text{Mb}] = 2\sigma[\text{Mb au}]/(\pi \text{FWHM}[\text{au}])$ where $\sigma[\text{Mb au}] = 2\pi^2 \alpha a_0^2 f[\text{au}] = 4.032 f[\text{au}]$.

In figure 3(b) there are two strong peaks at 28.4 eV and 29.9 eV and a broad structure in the range between 31 and 32 eV. A comparison with the measured satellite cross sections shows peaks for various satellite states at the same energies (see figures 2, 4, 5). Furthermore, the 4s ionization cross section (figure 3(a)) shows structures at these energies, too. Thus we suggest that the structures at 28.4 eV are due to autoionization of Kr I $4p^4(^1S)5s(^2S)5p$ doubly excited states and the structures at 29.9 eV due to autoionization of Kr I $4p^4(^1D)4d(^2P)5p$ and Kr I $4p^4(^1D)4d(^2D)5p$ states.

The magnitude of the calculated excitation cross sections of doubly excited states (figure 3(b)) is by no means represented by the sum of the peaks in the satellite cross sections and the 4s ionization cross section. There may be three reasons accounting for this disagreement.

(i) The decrease of Coulomb interaction (see section 3.3) will cause a decrease in the calculated excitation cross section of the doubly-excited states. This decrease was not included in the calculations up to now.

(ii) Some fraction of the populated doubly excited states may autoionize to the Kr II $4p^5\ ^2P_{1/2,3/2}$ ground state which is not observable by fluorescence spectroscopy. Branching ratio calculations for the autoionizing doubly excited states are needed for a direct comparison.

(iii) Interference effects between autoionizing states and the continuum (Fano 1961, Combet-Farnoux 1982) were neglected in the present calculations.

5. Summary

Absolute cross section measurements by means of PIFS were presented for the Kr 4s electron ionization in the threshold range with an exciting-photon bandwidth of 150 meV. Similar to results for other rare gases, the cross section is strongly structured because of autoionization processes of Kr I doubly excited states. For the first time absolute cross sections for the population of various Kr II satellite levels, too, were measured near threshold. These cross sections were dominated by the autoionization of Kr I doubly excited states. Furthermore, the fluorescence branching ratios of some satellite states to the Kr II $4s^24p^5\ ^2P_{1/2}$ and $^2P_{3/2}$ ground states were experimentally determined.

The experimental cross sections were compared with cross sections calculated. These calculations were carried out—as a first step towards a correct description—by neglecting the influence of the autoionization of doubly excited states. For a qualitative comparison, however, the excitation cross sections for doubly excited Kr I states were calculated. Using these cross sections some main features of the measurements were tentatively identified.

Acknowledgements

VLS and BML gratefully acknowledge support by the Sonderforschungsbereich 91 of the Deutsche Forschungsgemeinschaft during their stay at Kaiserslautern. HS, AE, FV, KHS and BM would like to thank the staff of BESSY for the continuous support during

the measurements. This work was funded by the German Federal Minister for Research and Technology under contract nos 05 452AXI and 05 5UKAXB 9.

References

Amusia M Ya and Cherepkov N A 1975 *Case Stud. At. Phys.* **5** 47–121
Aksela S, Aksela H, Levasalmi M, Tan K H and Bancroft G M 1987 *Phys. Rev.* A **35** 3449–50
Bauche J, Bauche-Arnould C and Klapish M 1988 *Adv. At. Mol. Phys.* **23** 131–95
Becker U, Hölzel R, Kerkhoff H G, Langer B, Szostak D and Wehlitz R 1986 *Phys. Rev. Lett.* **56** 120–3
Bethe H and Salpeter E 1957 *Quantum Mechanics of One- and Two-Electron Atoms* (Berlin: Springer)
Carter S L and Kelly H P 1977 *Phys. Rev.* A **16** 1525–34
Codling K and Madden R P 1971 *J. Res. NBS* A **76** 1–12
Combet-Farnoux F 1982 *Phys. Rev.* A **25** 287–303
Demekhin V F, Sukhorukov V L, Shelkovich T V, Yavna S A, Yavna V A and Bairachny Yu I 1979 *J. Struct. Chem (USSR)* **20** 38–48
Fano U 1961 *Phys. Rev.* **124** 1866–78
Hall R I, Avaldi L, Dawber R, Rutter P M, MacDonald M A and King G C 1989 *J. Phys. B: At. Mol. Opt. Phys.* **22** 3205–16
Hall R I, Avaldi L, Dawber G, Zubek M and King G C 1990 *J. Phys. B: At. Mol. Opt. Phys.* **23** 4469–85
Hall R I, Dawber G, Ellis K, Zubek M, Avaldi L and King G C 1991 *J. Phys. B: At. Mol. Opt. Phys.* **24** 4133–46
Huang K N, Johnson W R and Cheng K T 1981 *At. Nucl. Data Tables* **26** 33–45
Karazija R 1991 *Sums of Atomic Quantities and Mean Characteristics of Spectra* (Vilnius: Mokslas)
Kelly R L 1987 *J. Phys. Chem. Ref. Data* **16** suppl. 1
Kennedy D J and Manson S T 1972 *Phys Rev.* A **5** 227–47
Lindle D W, Heimann P A, Ferret T A, Piancastelli M N and Shirley D A 1987 *Phys Rev.* A **35** 4605–10
Möbus B 1988 *Diploma thesis* I Physikalisches Institut, University of Giessen
Moore C E 1971 *Atomic Energy Levels* NBS Circular No 467 (Washington, DC: US Govt Printing Office)
Petrov I D and Sukhorukov V 1991 *Today and Tomorrow in Photoionization* ed M Ya Amusia and J B West (DL/SCI/R29 Daresbury Laboratory) pp 187–93
Rajnak K and Wybourne B G 1963 *Phys. Rev.* **132** 280–90
Samson J A R and Gardner J L 1974 *Phys. Rev. Lett.* **33** 671–3
Schartner K H, Lenz P, Möbus B, Schmoranzer H and Wildberger M 1989 *J. Phys. B: At. Mol. Opt. Phys.* **22** 1573–81
Schartner K H, Magel B, Möbus B, Schmoranzer H and Wildberger M 1990 *J. Phys. B: At. Mol. Opt. Phys.* **23** L527–32
Schartner K H, Möbus B, Lenz P, Schmoranzer H and Wildberger M 1988 *Phys. Rev. Lett.* **61** 2744–7
Schartner K H, Möbus B, Wildberger M, Ehresmann A and Schmoranzer H 1991 *BESSY annual report 1991* p 514
Schmoranzer H, Wildberger M, Schartner K H, Möbus B and Magel B 1990 *Phys. Lett.* **150A** 281–5
Sevier K D 1979 *At. Data Nucl. Data Tables* **24** 323–71
Striganov A R and Sventitskij N S 1968 *Tables of Sectral Lines of Neutral and Ionized Atoms* (New York/Washington: IFI/Plenum)
Sukhorukov V L, Lagutin B M, Schmoranzer H, Petrov I D and Schartner K H 1992 *Phys. Lett.* **169A** 445–51
Sukhorukov V L, Petrov I D, Demekhin V F and Lavrent'ev S V 1985 *Bull Akad. Sci. USSR* **49** 1463–70
Sukhorukov V L, Petrov I D, Lavrent'ev S V and Demekhin V F 1991 *Today and Tomorrow in Photoionization* ed M Ya Amusia and J B West (DL/SCI/R29 Daresbury Laboratory) pp 7–14
Wijesundera W and Kelly H P 1989 *Phys. Rev.* A **39** 634–43
Wills A A, Cafolla A A and Comer J 1990a *J. Phys. B: At. Mol. Opt. Phys.* **23** 2029–36
Wills A A, Cafolla A A, Curell F J, Comer J, Svensson A and MacDonald M A 1989 *J. Phys. B: At. Mol. Opt. Phys.* **22** 3217–26
Wills A A, Cafolla A A, Svensson A and Comer J 1990b *J. Phys. B: At. Mol. Opt. Phys.* **23** 2013–28